

THEORETICAL APPROACH TO SINGLE-MODE OPERATION OF BISTABLE FABRY-PEROT LASER CONTAINING SATURABLE ABSORBER

Phung Quoc Bao, Dinh Van Hoang

Department of Physics, Colledge of Science - VNU

Abstract: *A theoretical approach to the optical bistability (OB) effect in single-mode Fabry-Perot lasers containing saturable absorber (LSA) is presented on the basis of the rate equations with allowance for spontaneous emission and spatial hole-burning. Special attention is paid to the case of dominant inhomogeneous broadening in both Lorentzian and Gaussian models. The influence of the main LSA parameters on OB occurrence conditions as well as on OB curves' characteristics are investigated in detail.*

Made to operate in two stable low and high output levels corresponding to the unsaturated and strongly saturated states of the intracavity absorber, a laser containing saturable absorber (LSA) may exhibit a hysteresis cycle of photon density versus laser pumping power (see [1-4], for instance). This bistable operation results from the combined effect of the saturable absorber and the feedback provided by the optical cavity itself. The OB features are therefore dependent not only on the LSA parameters but on the cavity geometry of LSA as well. Recently, in [5-7] has been performed a systematic analysis for OB of dominant inhomogeneously broadened ring LSA. This paper is devoted to investigate the OB behavior of Fabry - Perot LSA when the inhomogeneous atomic linewidth greatly exceeds the homogeneous one. Both Lorentzian and Gaussian laser pumping rate profiles are taken into account in the rate equations with allowance for spontaneous emission and spatial hole burning.

Our LSA model consists of a planar-mirror Fabry - Perot resonator of length L , directed along the x -axis, containing the amplification and absorption cells with the same length l at the coordinates x_a and x_b , respectively. Both amplifier and absorber are considered as ensembles of two-level atoms whose atomic line-widths are assumed to be of Lorentzian homogeneously broadened with the same half-width Γ . The inhomogeneous gain profile of half-width ϵ centered at Ω_0 is composed of a continuous distribution of homogeneous packets at frequencies ω_μ . We consider the case where the cavity can sustain only one mode of photon number n_j with circular frequency $\Omega_j = \pi m_j c/L$ (m_j integer, c velocity of light) at a detuning $\Delta_j = |\Omega_j - \Omega_0|$. For simplicity, we assume the cavity losses χ_j in this mode to be constant. In the rate equation approximation, such a system obeys the following equations:

$$\frac{dn_j}{dt} = -\chi_j n_j + 2hB(n_j + 1) \sum_{\mu} g(\omega_{\mu} - \Omega_j) [N_{\mu a}^h - N_{\mu b}^h], \quad (1.a)$$

$$\frac{dN_{\mu a}^h}{dt} = R_{\mu a} - [hBg(\omega_{\mu} - \Omega_j)n_j + \gamma_a] N_{\mu a}^h, \quad (1.b)$$

$$\frac{dN_{\mu b}^h}{dt} = R_{\mu b} - [hBg(\omega_\mu - \Omega_j)n_j + \gamma_b]N_{\mu b}^h \quad (1.c)$$

with $h=3/4$.

Here B is the Einstein coefficient and $g(\omega_\mu - \Omega_j)$ can be generally represented by a function of the form:

$$g(\omega_\mu - \omega) = \frac{\Gamma^2}{\Gamma^2 + 4(\omega_\mu - \omega)^2} \quad (2)$$

$N_{\mu i}^h \equiv N_{\mu i} - N_{\mu ij}$ are effective population differences in both media with:

$$N_{\mu i} = \int_{x_i - \frac{1}{2}}^{x_i + \frac{1}{2}} n_{\mu i}(x, t) dx \quad \text{and} \quad N_{\mu ij} = \int_{x_i - \frac{1}{2}}^{x_i + \frac{1}{2}} n_{\mu i} \cos\left(\frac{2\pi m_j x}{L}\right) dx \quad (3)$$

(here i stands for a or b).

$n_{\mu a}(x, t)$ and $n_{\mu b}(x, t)$ are the densities of population differences between the atomic upper and lower levels in both media. γ_a and γ_b denote the relaxation rates of the upper levels in the amplifying and absorbing atoms, respectively.

In the Lorentzian model, the laser pumping rate $R_{\mu a}$ with the pumping rate constant R_0 can be expressed as follows:

$$R_{\mu a} = R_0 \frac{\epsilon}{\epsilon^2 + 4(\omega_\mu - \Omega_0)^2}. \quad (4)$$

As for the Gaussian model, it can be written as:

$$R_{\mu a} = GR_0 \exp\left[-\frac{4(\omega_\mu - \Omega_0)^2 \ln 2}{\epsilon^2}\right] \quad \text{with} \quad G = \sqrt{\pi \ln 2}. \quad (5)$$

The absorber-pumping rate $R_{\mu b}$ is assumed to be constant.

The calculations in detail show that this rate equation approximation is easily justified in the case of steady-state operation near threshold when the photon number in Fabry - Perot LSA is not larger than 4.10^{11} .

Setting the time derivatives in Eqs.(1) equal to zero and evaluating the sum over μ by the transformation given below [5]:

$$\sum_{\mu} f(\omega_{\mu}) \Rightarrow \frac{1}{\pi \epsilon} \int_{-\infty}^{+\infty} f(\omega) d\omega \quad (6)$$

we obtain the Lorentzian steady-state equation:

$$Q_j - h\alpha \left(Q_j + \frac{B}{\gamma}\right) \left[\frac{\sigma_0}{\sqrt{1 + hQ_j} [1 + \alpha \sqrt{1 + Q_j} + 4\delta_j^2 (1 - \alpha \sqrt{1 + Q_j})]} - \frac{\sigma_b}{\xi \sqrt{1 + hQ_j/\xi}} \right] = 0 \quad (7)$$

and the Gaussian one:

$$Q_j - \frac{\alpha}{4} \left(Q_j + \frac{B}{\gamma}\right) \left[\frac{G\sigma_0 \text{Re}W(2\delta_j \sqrt{\ln 2} + i\alpha \sqrt{(1 + hQ_j) \ln 2})}{\sqrt{1 + hQ_j}} - \frac{\sigma_b}{\xi \sqrt{1 + hQ_j/\xi}} \right] = 0, \quad (8)$$

where $Q_j = \frac{B}{\gamma} n_j$ - j^{th} mode intensity with $\gamma = \gamma_a$;

$$\sigma_0 = \frac{B R_0}{\gamma \chi_j} - \text{laser pumping rate};$$

$$\xi = \frac{\gamma_b}{\gamma} - \text{saturation coefficient};$$

$$\alpha = \frac{\Gamma^a}{\Gamma} - \text{ratio of homogeneous to inhomogeneous broadening};$$

$$\sigma_b = \frac{B R_{pb}}{\gamma \chi_j} - \text{absorber pumping rate};$$

$$\delta_j = \frac{\Delta_j}{\epsilon} - \text{detuning scaled to the inhomogeneous half-width.}$$

$W(z)$ - the error function of complex argument z - which is defined by [8]:

$$W(z) = \exp(-z^2) \operatorname{erfc}(-iz) \quad \text{with} \quad \operatorname{erfc}(-iz) = 1 + \frac{2i}{\sqrt{\pi}} \int_0^z e^{-t^2} dt. \quad (9)$$

Slightly above the laser threshold, Eqs. (7) and (8) can be approximated by a cubic equation of the form:

$$a_0 Q_j^3 + a_1 Q_j^2 + a_2 Q_j + a_3 = 0, \quad (10)$$

where:

$$\begin{aligned} a_0 &= h^2 [(1 + 2a\alpha)(1 - 4b\delta_j^2) + 8b\delta_j^2] \\ a_1 &= 2h \{ [(1 + a\alpha)(1 + \xi) + a\xi\alpha](1 - 4b\delta_j^2) + 8b\delta_j^2(1 + \xi) \} + \dots \\ &\quad \dots + \frac{h\alpha}{2} \{ \sigma_b [(1 + 2a\alpha)(1 - 4b\delta_j^2) + 8b\delta_j^2] - G\sigma_0 \} \\ a_2 &= (4\xi + \alpha\sigma_b) [(1 + a\alpha)(1 - 4b\delta_j^2) + 8b\delta_j^2] - \alpha\xi G\sigma_0 \\ a_3 &= \alpha \frac{B}{\gamma} \{ \sigma_b [(1 + a\alpha)(1 - 4b\delta_j^2) + 8b\delta_j^2] - \xi G\sigma_0 \} \end{aligned}$$

with $a = b = 1$ for the Lorentzian pumping profile and $a \approx 0.95, b \approx -0.80$ for the Gaussian pumping profile.

The numerical analysis of Eq.(10) shows that at a given δ_j , for a appropriate control parameter set (ξ, α, σ_b) , the OB may occur in a certain range of laser pumping rate σ_0 confined between σ_{0m} and σ_{0M} . By definition, the OB curve's characteristics are OB onset value σ_{0m} , OB width (the difference $\sigma_{0M} - \sigma_{0m}$) and OB height (the LSA photon intensity at σ_{0M}).

In resonance ($\delta_j = 0$), for given values of $(\xi\alpha)$, no OB action is observed until the absorber pumping rate reaches a minimum value σ_{bm} . Increasing σ_b , the typical full-shaped OB curve is shifted towards the higher laser pumping rates, at the same time it's size get larger. Just as σ_b goes beyond a critical value σ_{bt} , a portion of the OB lower branch becomes negative, thus physically meaningless, and hence the OB curve is partly truncated away. Further increasing σ_b , the truncated OB curve is always displaced towards higher σ_0 , the OB height grows continuously, but the effective OB width remains constant. The resonant OB phase diagram divides the (ξ, α) parameter plan into three domains (from left to right): mono-stable, bistable, and truncated bistable (Fig.1).

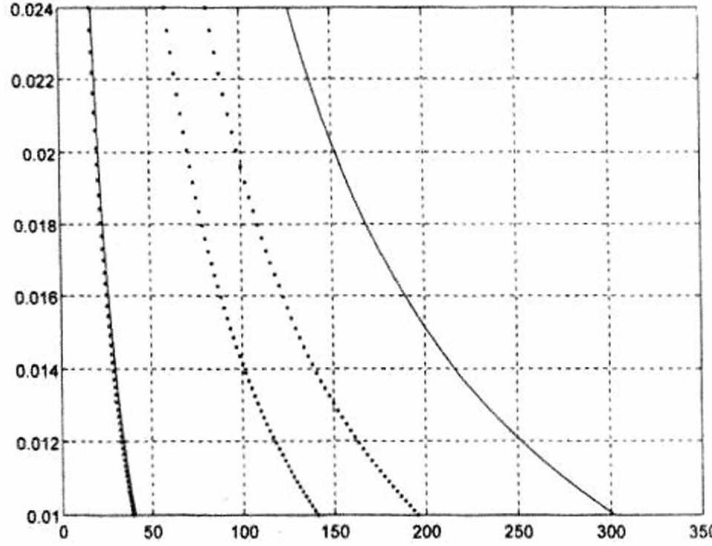


Fig. 1. Lorentzian OB phase diagram in resonance ($\delta_j = 0$, solid lines), in non-resonance ($\delta_j = 0.294$, dotted lines)

In non-resonance ($\delta_j \neq 0$), for given values of (ξ, α) , there exist also the two critical absorber pumping rates σ_{bm} and σ_{bt} . However, the more the LSA is detuned, the smaller the possible full-shaped OB parameter region $\sigma_{bt} - \sigma_{bm}$. Moreover, as σ_b increases past σ_{bt} , the effective OB width diminishes quickly and vanishes at a certain value σ_{boff} . The OB action is off. The larger the detuning δ_j , the more rapidly the effective OB decreases. The non-reasonable OB phases diagram divides now the (ξ, α) parameter plan into four domains: monostable, bistable, truncated bistable and OB-off (Fig. 1). Nearly the same size in resonance, the Lorentzian OB parameter domains reduce more quickly than the Gaussian ones by increasing the detuning δ_j . The OB width variations for a set of values (ξ, α) in both resonant and non-resonant Gaussian LSA are depicted in Fig. 2. The Gaussian OB width is always smaller than the Lorentzian one of the same parameter set.

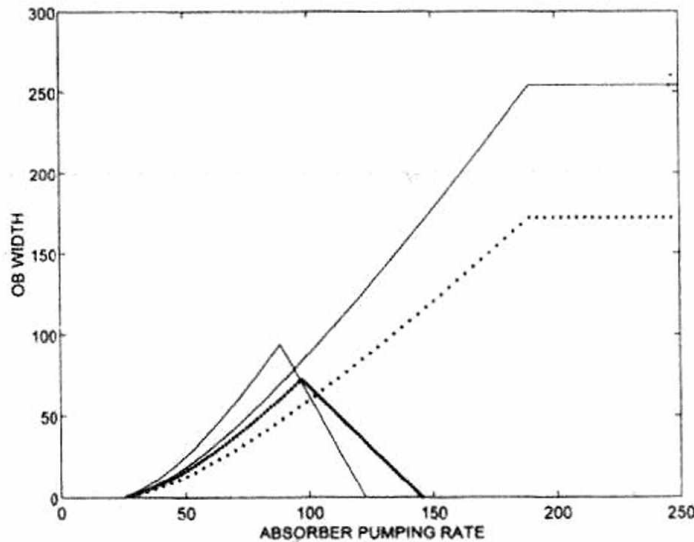


Fig. 2. Lorentzian (solid lines) and Gaussian (dotted lines) OB width variations for $\xi = 0.25, \alpha = 0.016$ at various detuning values

To perform the linear stability analysis of the steady-state solutions n_{js} , $N_{\mu as}^h$ and $N_{\mu bs}^h$ for an appropriate set of parameter values, we start with Eqs.(1) and let:

$$n_j(t) = n_{js} + \eta_j e^{-\lambda t}; \quad N_{\mu a}^h(t) = N_{\mu as}^h + \eta_{\mu a} e^{-\lambda t} \quad N_{\mu b}^h(t) = N_{\mu bs}^h + \eta_{\mu b} e^{-\lambda t}. \quad (11)$$

Linearizing the obtained equations with respect to the assumedly real fluctuations $\eta_j, \eta_{\mu a}, \eta_{\mu b}$, we arrive at a system of linear homogeneous algebraic equations. In order that there exists a nontrivial solution, the associated determinant should vanish:

$$\det(A + \lambda I) = 0 \quad (12)$$

where I is the unity matrix and A - a matrix with the following elements:

$$\begin{aligned} a_{11} &= -\chi_j + 2hB \sum_{\mu=-\infty}^{+\infty} g(\omega_\mu - \Omega_j)(N_{\mu a}^h - N_{\mu b}^h)|_s; \quad a_{12} = -a_{13} = \frac{\alpha B(n_{js} + 1)}{2}|_s \\ a_{21} &= -B\bar{g}N_{\mu as}^h; \quad a_{22} = -B\bar{g}n_{js} - \gamma; \quad a_{23} = 0 \\ a_{31} &= -B\bar{g}N_{\mu bs}^h; \quad a_{32} = 0; \quad a_{33} = -B\bar{g}n_{js} - \xi\gamma, \end{aligned}$$

here \bar{g} is the average value within the frequency range of 2Γ centered at Ω_j . And this furnishes an equation for λ :

$$\begin{aligned} \lambda^3 - b_2\lambda^2 + b_1\lambda - b_0 &= 0, \quad (13) \\ b_0 &= a_{12}a_{21}a_{33} - a_{11}a_{22}a_{33} - a_{12}a_{21}a_{31} \\ b_1 &= a_{12}a_{22} + a_{11}a_{33} + a_{22}a_{33} + a_{12}a_{31} - a_{12}a_{21} \\ b_2 &= -(a_{11} + a_{22} + a_{33}). \end{aligned}$$

According to the expanded Routh - Hurwitz theorem, all the real parts of the roots λ_i of Eq.(13) are positive, that implies the corresponding steady-state solutions are stable, provided that $b_0 > 0$, $b_1b_2 - b_0 > 0$ and $b_2 > 0$.

The stability of the resonant hysteresis curves is numerically checked with $\chi_j = 10^{-2}s^{-1}$, $B = 10^{-3}s^{-1}$ and $\gamma = 10^8s^{-1}$ [5]. Some results are displayed in Fig.3. The point and plus (or x for Gaussian curves) marks represent unstable and stable solutions, respectively. The whole middle branch is always unstable, whereas the lower and upper branches steadily exhibit the stability for every set of parameter values. This is not the case in resonant ring LSA where there may exist an instability section on the OB upper branch just after the turning point [7].

For given (ξ, α, σ_b) in the bistable phase domain, the stability analysis of the non-resonant steady-state solutions shows that there exists a certain detuning at which a section of the OB upper branch, just after the turning point, becomes unstable. The more the LSA is detuned, the more the instability section extends towards higher pumping rates (Fig. 4). The critical detuning for $(\xi = 0.25, \alpha = 0.16, \sigma_b = 40)$ is about 0.075 and 0.148 in Lorentzian and Gaussian LSA, respectively. For the same set (ξ, α) as before, we fix at $\delta_j = 0.176$ and carry out the stability analysis of the truncated OB curves with various

σ_b . By increasing σ_b , the OB curves are more and more truncated but still remain the same stability properties as in resonance (Fig. 5).

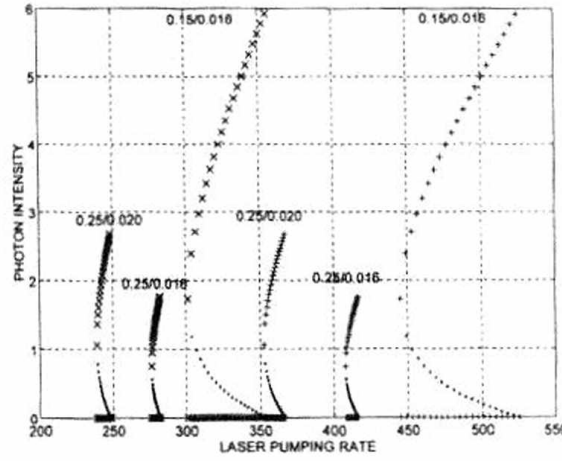


Fig.3. Stability of resonant Lorentzian (+) and Gaussian (x) OB curves for $\sigma_b = 40$ at various sets of (ξ/α)

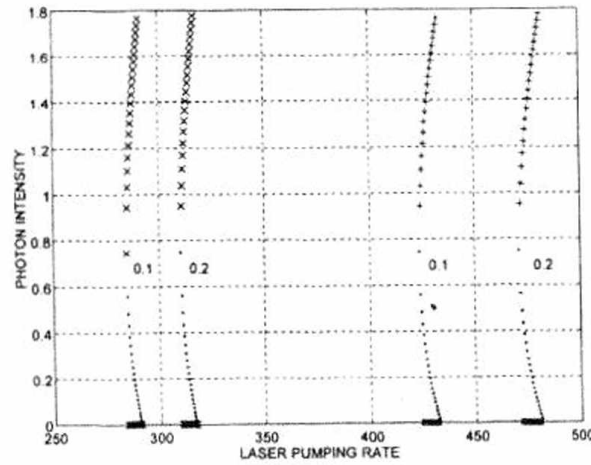


Fig.4. Stability of non-resonant Lorentzian (+) and Gaussian (x) OB curves for $\xi = 0.25, \alpha = 0.016, \sigma_b = 40$ at various detuning values

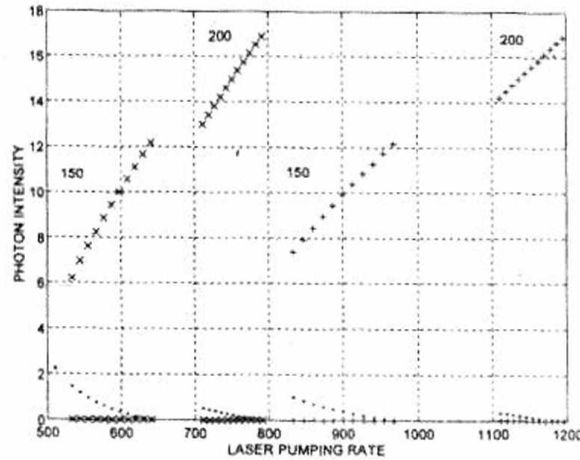


Fig.5. Stability of non-resonant truncated Lorentzian (+) and Gaussian (x) OB curves for $\xi = 0.25, \alpha = 0.016$ at various absorber pumping values

We have presented a theoretical approach to OB behavior of single-mode Fabry - Perot LSA with dominant Lorentzian/Gaussian inhomogeneous broadening in both resonance and non-resonance cases. The control parameters conditions for OB occurrence become more strict as soon as LSA is detuned. Once OB occurred, one can enlarge the OB curve's shape by choosing small ξ and large α, σ_b . At high values of σ_b , OB curves may have a truncated form. The linear stability analysis in resonant LSA has shown two of three steady state solutions are always stable and no instability on the OB upper branch is observed. This gives rise to a full hysteresis loop of the photon density versus the laser pumping rate. When the LSA is detuned by an amount large enough, there appears an upper-branch instability section, which slightly reduces the calculated hysteresis loop. It is worth noticing that in comparison with the Lorentzian model, the Gaussian LSA may have a larger OB parameter region, a smaller OB onset value and higher control efficiency. Furthermore, Gaussian hysteresis curves are more stable against accidental changes of the LSA detuning. From the practical viewpoint, a Gaussian resonant LSA may be the most favorable to OB operation as far as the used approximation holds.

References

1. R. Muller. *Z. Physik B- Condens. Matter*, **40**(1980), 257.
2. L. A. Lugiato and L. M. Narducci. *Phys. Rev.*, **A32**(1985), 1576.
3. D. Dangoisse, P. Glorieux and D. Hennequin., *Phys. Rev.* **A42**(1990), 1551.
4. Dinh Van Hoang and Tran Thi Thu Ha, *Inf. Phys.* **32**(1991), 75.
5. Phung Quoc Bao and Dinh Van Hoang, *Proc. of 7th Asia Pacific Phys. Conf.*, Beijing, China. 1997, 445.
6. Phung Quoc Bao and Dinh Van Hoang, *Comm. in Phys.*, CNST, 8, No.1(1998), 33.
7. Dinh Van Hoang and Phung Quoc Bao, *Proc. of 2th Nat. Conf. on Optics and Spectroscopy*, Thainguyen, Vietnam, 1998.
8. M. Abramowitz and I. Stegun. *Handbook of Mathematical Functions*, Dover, New York, 1972.

TẠP CHÍ KHOA HỌC ĐHQGHN, Toán - Lý, T.XVIII, Số 2 - 2002

MỘT CÁCH TIẾP CẬN LÝ THUYẾT VỀ HOẠT ĐỘNG ĐƠN MODE LUỒNG ỔN ĐỊNH CỦA LASER FABRY - PEROT CHỨA CHẤT HẤP THỤ BẢO HOÀ

Phùng Quốc Bảo, Đinh Văn Hoàng

Khoa Vật lý, Đại học Khoa học Tự nhiên - ĐHQG Hà Nội

Bài báo trình bày một cách tiếp cận lý thuyết hiệu ứng lưỡng ổn định quang học (OB) trong laser Fabry - Perot đơn mode, chứa chất hấp thụ bão hòa (LSA) dựa trên gần đúng phương trình tốc độ có tính đến bức xạ tự phát và sự tạo hốc không gian. Các trường hợp mở rộng không đồng nhất dạng Lorentz và dạng Gauss được đặc biệt chú ý. Ảnh hưởng của các tham số LSA lên điều kiện xuất hiện cũng như lên đặc trưng của đường cong lưỡng ổn định được nghiên cứu chi tiết.